Phasing metrology system for the GMT

D. Scott Acton[1], Antonin Bouchez[2]

[1]Ball Aerospace and Technologies Corporation, 1600 Commerce Street, Boulder, CO 80501
[2]Giant Magellan Telescope, 251 Lake Street, Suite 300, Pasadena, CA 91101

ABSTRACT

The Giant Magellan Telescope (GMT) is a 25.4 m diameter ground-based segmented Gregorian telescope, composed of 7 8.4 meter diameter primary mirror segments, and 7 1 meter diameter adaptive secondary mirror segments. Co-phasing of the integrated optical system will be partially achieved by making real-time measurements of the wavefront of an off-axis guide star. However, slowly varying aberrations due to thermal and gravitational effects, as well as wind buffeting, will make it difficult to maintain alignment using real-time optical measurements alone. Consequently, we are proposing internal metrology systems to maintain the relative alignment of the optical elements. In this paper we describe a differential capacitive edge sensing system to maintain the relative alignment of the adaptive secondary mirror reference bodies. We also propose an interferometric system for sensing of the relative displacements of primary mirror segments.

Keywords: Extremely Large Telescopes, Wavefront Sensing and Controls

1. INTRODUCTION

The GMT is an extremely large, segmented Gregorian telescope, which will be constructed on Cerro Las Campanas in Chile. A notional drawing of the GMT is shown in Figure 1. The primary mirror (M1) consists of 7 8.4-meter diameter circular segments (shown on the left). The secondary mirror (M2) is identically segmented (shown on the right), consisting of 7 1 meter round mirrors. Each of the primary and secondary mirror segments are mounted on hexapod positioners, capable of controlling the 6 rigid body motions to micron-level accuracy. The primary mirror segments also contain multiple force actuators for active control of the mirror figure. Likewise, each secondary mirror segment has hundreds of actuators for real-time adaptive correction of the atmospheric turbulence.

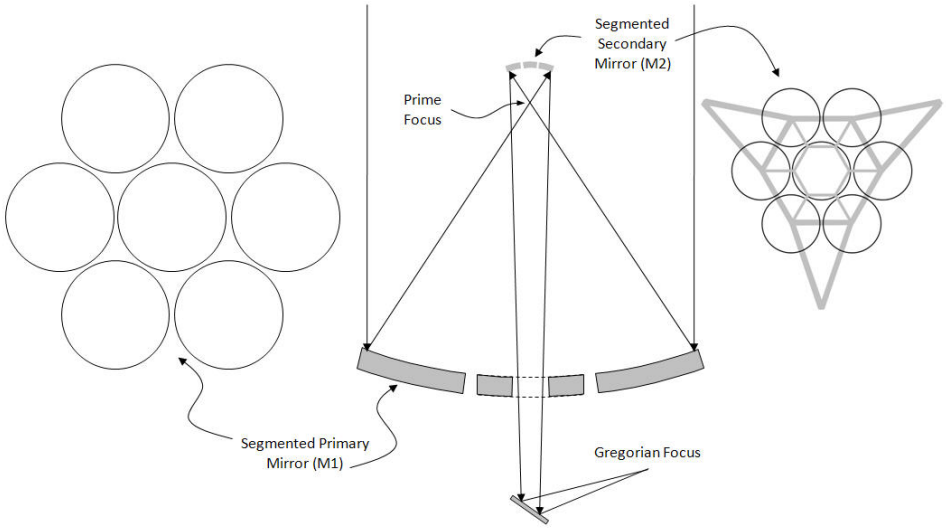

Figure 1. The Giant Magellan Telescope.

Closed-loop operation of the GMT will involve interactions between the adaptive optics, which correct the atmospheric turbulence, the active optics, which keep the telescope aligned, and optical sensors which establish and maintain the phasing of the telescope [1]. A detailed description of this interaction is beyond the scope of this paper. However, one of the key elements is the internal metrology systems which detect rigid-body motions of the outer mirror segments relative to center segments in both M1 and M2.

The metrology system for M1 must meet the following requirements:

- It must permit up to 3 cm of motion of any M1 segment, without creating a collision in the sensor components.
- It must facilitate rapid recovery of M1 segment positions, to within a few microns (absolute), after being shut down, or after an off-nominal event.
- It must be able to sense segment-level piston fluctuations to within about 10 nm (wavefront) which result from vibration and wind buffeting, at about 50-100 Hz.
- It must be stable in piston to better than the capture range of the AO wavefront sensors (200-300 nm, wavefront) for several minutes at a time, to support slewing to and acquiring new science objects.

Because the secondary mirror (M2) is concave, it is possible to place a calibration source at the prime focus, to stimulate a wavefront sensor at the Gregorian focus. Consequently, it should be relatively straightforward to co-align the M2 segments prior to initiating an observing session. The goal of the M2 metrology system will be to maintain this alignment throughout the observing session. Because the segments in M1 are also adjustable, one can conceive of scenarios where an optical error in M2 is compensated by a similar "error" in M1. For many optical aberrations, this is acceptable. Segment-level tilt, however is problematic because even a small amount will create a field-dependent piston term in the wavefront. In some observing modes, the nominal segment-level piston will be monitored with an off-axis piston sensor, resulting in an uncorrected piston error within the science field. Consequently, it is vital that the M2 metrology system be capable of maintaining relative tilt between the segments.

Specific requirements for the M2 metrology system are:

- Must fit in the small space afforded by the M2 structure.
- Must be located within the shadow of the M2 support structure (gray bars, right of Figure 1) as seen by M1 (to minimize thermal emissivity).
- Must not prevent the removal of an M2 segment.
- Should measure segment-level piston accurately to about 10 nm (wavefront) at speeds of 50-100 Hz.
- Must sense segment-level tilt to about 1.0 microradians stably over 12 hours.

The conceptual designs for the metrology systems are presented in the balance of this paper.

2. THE SENSORS

One of the most difficult challenges in building a metrology system for M1 is the need to allow for up to 3 cm motion between segments. Any sensor on an M1 segment must therefore be located at least 6 cm from hardware on an adjacent segment. Given that we must measure piston values on the order of 10 nm in the wavefront, we are motivated to use an interferometric type sensor, of which there are several commercial options. These sensors measure displacement changes by counting interference fringes in quadrature. If the beam is interrupted, the distance information is largely lost. Therefore, whenever lock is lost on a sensor/retro pair, the zero point has to be reestablished.

We propose a hybrid metrology system that supplements the interference based sensors with a more coarse sensor with larger capture range. The coarse sensors will make it possible to quickly establish wavefront sensing capture range (about 10 microns of piston error). Once the optical phasing has been achieved, we can then rely on the interferometric metrology system to maintain the phasing between optical sensor updates.

The space constraints of the M2 sensors, however, argue for capacitive edge sensors, which have considerable heritage for segmented telescopes [2].

2.1 M1 fine sensors

Our proposed fine sensor for the M1 metrology system is the Renishaw Distance Measuring Interferometer (DMI). Each sensor consists of a frequency-stabilized laser coupled to a 3-meter single-mode polarization-maintaining fiber. At the end of the fiber is a small interferometer head that projects the laser to a cube and reads the return signal. This is illustrated in Figure 2. The heads would be mounted to the side-walls of the M1 segments, with the electronics and lasers mounted in the cell below the M1 segments. If properly implemented, the DMI's should be able to sense ~1 nm length changes.

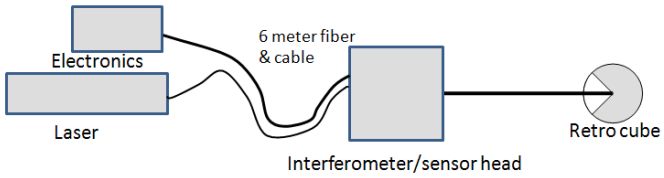

Figure 2. DMI.

2.2 M1 coarse sensors

For the M1 metrology system coarse sensor, we propose an absolute imaging encoder described in references [3] and [4], and illustrated in Figure 3. A special target is attached to the side-wall of an M1 segment. An image of the target is formed via a lens onto a simple 8-bit camera, mounted to an adjoining segment. The target is designed in such a way so that the camera (and its associated software) can know in an absolute sense where it is pointing, while still giving sub-micron sensitivity. As such, this type of encoder would have a capture range of several cm. The short-term sensitivity to translation is on the order of 0.2 microns, The long term sensitivity should be about 2 microns, limited by the stability of the detector/optics/segment interface.

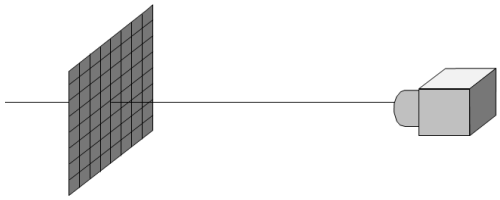

Figure 3. Absolute Imaging Encoder concept.

2.3 M2 sensors

For M2, we propose a sensor that uses a pair of differential capacitive plates, as illustrated in Figure 4. This sensor will permit the measuring of 6 different capacitances, which we denote with the letter "C":

- C(1,1a)
- C(1,1b)
- C(1,1a+1b)
- C(2,2a)
- C(2,2b)
- C(2,2a+2b)

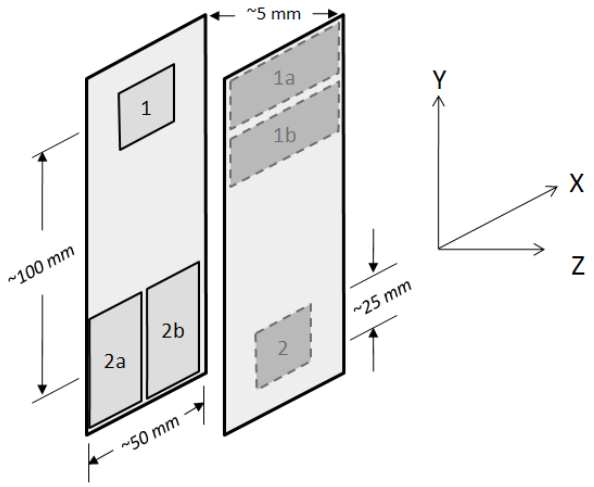

Figure 4. Differential capacitive edge sensor concept.

When the right-most half of the sensor is moved relative to the left-most half, the capacitance values change. Some modes can be sensed strongly; others not at all:

- ΔX derived from C(2,2a) – C(2,2b)
- ΔY derived from C(1,1a) – C(1,1b)
- ΔZ derived from C(1,1a+1b) + C(2,2a+2b)
- θX derived from C(1,1a+1b) – C(2,2a+2b)
- θY not observed
- θZ not observed

(Note that θ refers to rotation about the specified axis.) We can estimate the sensitivity of the differential sensor by first establishing the sensitivity of a hypothetical capacitor with 25 X 25 mm plates, separated by 5 mm. We could appeal to basic physics to establish the initial sensitivity. For this conceptual design, however, it will be sufficient to estimate the sensitivity from commercially available products, noting that in a rough sense,

- The sensitivity increases linearly with the plate area
- The sensitivity decreases linearly with separation
- The sensitivity decreases with the square-root of the temporal bandpass

In Table 1, we have picked the closest matching product from 3 different manufacturers, and estimated the performance of our hypothetical capacitor. (Note that this involves a bit of extrapolation, so these predictions should only be considered estimates.)

	Queensgate	Physik-Instrumente	Micro-Epsilon
Model	NXD	D-100.00	CS-05
Plate area (mm^2)	282	113.1	125
Spacing (mm)	1.25	0.3	5.0
Estimated Noise at 50Hz	1.3 nm RMS	0.2 nm RMS	0.6 nm RMS
Implied sensitivity of GMT capacitor	2.3 nm RMS	0.6 nm RMS	0.125 nm RMS

Table 4. Comparison of three commercial products with the hypothetical capacitor.

We will take the middle value of 0.6 nm RMS at 50 Hz for the assumed sensitivity of our hypothetical capacitive sensor. We can use this value to estimate the sensitivity for measuring each degree of freedom of our proposed sensor in Fig. 4.

ΔX, ΔY

ΔX and ΔY are actually differential measurements obtained by splitting the small plate in half, and comparing the change in capacitance on one half to that of the other (Figure 5). This cuts the sensitivity in half as well. However, the final translation is determined by combining two uncorrelated signals, which gives us an *increase* of sqrt(2) in sensitivity, for a net decrease of sqrt(2). The sensitivity for these measurements is therefore 0.85 nm rms.

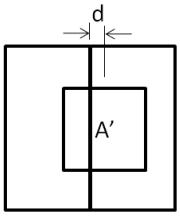

Figure 5. Differential measurements.

ΔZ

Displacement along the Z axis is derived from 4 uncorrelated capacitance measurements. This should give us an *improvement* of 2x in the sensitivity. However, they are made with plates cut in half, so we lose this sensitivity and we are back to 0.6 nm rms.

θX

This is very similar to the ΔZ measurement, except we need to subtract the top result from the bottom. Consequently, we are differencing two results instead of averaging, and we lose a factor of sqrt(2) in sensitivity instead of gaining it. The result is 1.2 nm acting over a distance of about 100 mm, which in turn gives us an angular sensitivity of about 12 nanoradians.

3. SENSOR LOCATIONS

Our proposed layout of sensors for M1 is illustrated in Figures 6, 7 and 8. Suites of sensors are mounted at 24 locations. The separation between segments at this location is ~600 mm. Two fine sensors and 1 coarse sensor are required at each location on M1. As shown in Figure 7, two fine sensors form a criss-cross pattern across an M1 segment boundary. A coarse sensor, however, simply looks at its associated target on an adjoining segment. The two cameras at each segment interface are mounted with a 20-degree angle between them, so that absolute displacement between the segments can be sensed.

The proposed sensor layout for M2 is shown on the left of Figure 9. Note that only 1 sensor is used per segment interface, for a total of 12 sensors.

4. SYSTEM MATRICES

The sensors have been arranged so that each outer segment has the same geometry, relative to segment-local coordinates which rotate with the segment position (Figures 5, 6, and 9). As a result, we only need to calculate how the sensed values will change on a single segment in response to the usual 6 degrees of freedom of motion, relative to the center segment. On M1, sensors were assumed to be located at the natural segment boundaries, with a 20 degree angle between each half. For the fine sensors in M1, we are simply measuring the change of length between the retro cubes and the sensor head in response to these motions. Once the locations are known, therefore, simple geometry can be used to calculate the change length in response to the applied mode change. The resulting response is shown for the fine sensors in Table 1. The units are microns of length change per micron or microradian of motion of the segment.

In a similar manner, the image motions in response to a pose change can be worked out for the coarse sensor geometry. In this case, we adopt a right-hand coordinate system on the target, as seen from the perspective of the camera. The Y axis will always be out of the page. We will define the image motion as the motion of the chief ray of the camera optics as it hits the target. The results are shown in Table 2. R is the radius of a segment, which is 4.2 meters.

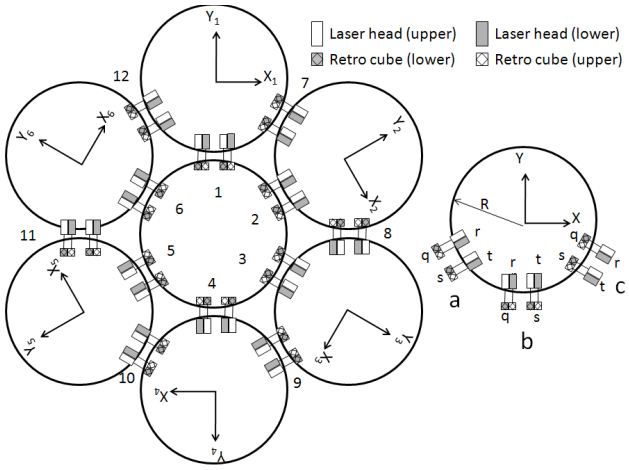

Figure 6. Locations of the M1 fine sensors. A total of 48 DMIs are used.

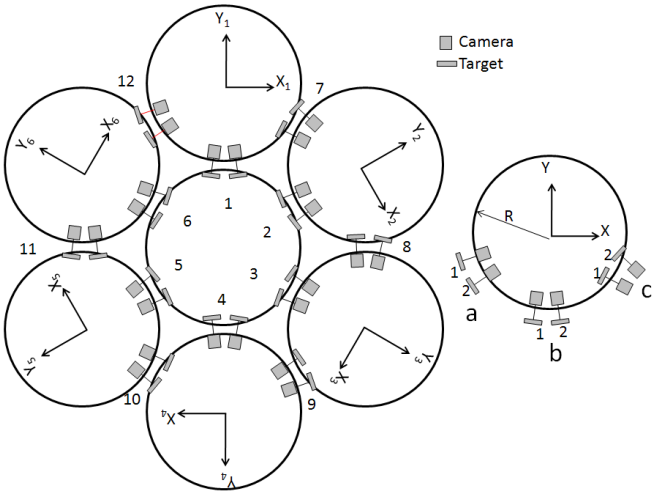

Figure 7. Locations of the M1 coarse sensors. A total of 24 cameras are used.

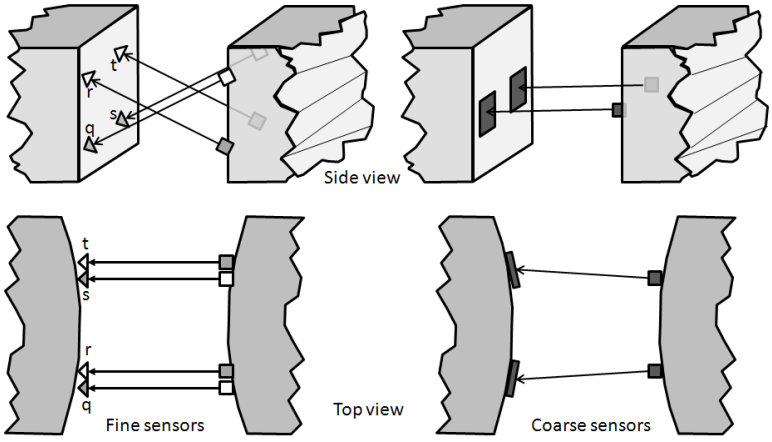

Figure 8. Coarse and fine sensor geometry for M1.

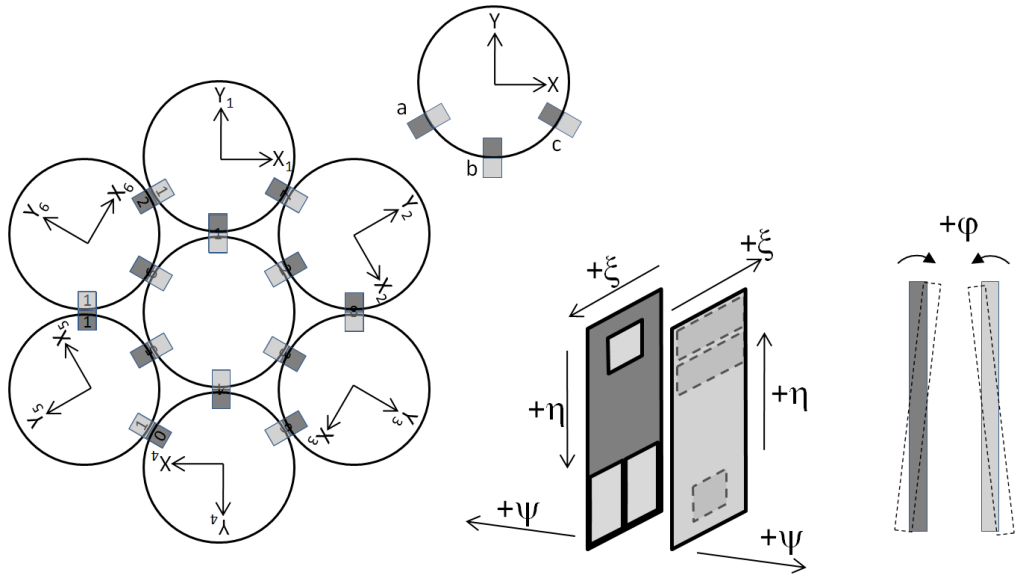

Figure 9. Left: M2 sensor location. Right: local sensor coordinate system.

	a				b				c			
Mode	q	r	s	t	q	r	s	t	q	r	s	t
X-tran	0.67	0.67	0.61	0.61	-0.01	-0.01	0.01	0.01	-0.61	-0.61	-0.66	-0.66
Y-tran	0.36	0.36	0.44	0.44	0.79	0.79	0.79	0.79	0.44	0.44	0.36	0.36
Piston	0.66	-0.66	0.66	-0.66	0.61	-0.61	0.61	-0.61	0.66	-0.66	0.66	-0.66
Theta-X	-0.93	0.93	-1.79	1.79	-2.50	2.52	-2.50	2.52	-1.79	1.79	-0.93	0.93
Theta-Y	2.60	-2.59	2.11	-2.10	0.45	-0.45	-0.45	0.45	-2.10	2.11	-2.59	2.60
Theta-Z	0.49	0.49	-0.26	-0.26	0.65	0.65	-0.63	-0.63	0.29	0.29	-0.46	-0.46

Table 1: Response of a pose change of a local segment, relative to its neighbors. Units are microns of length change per micron (or microradian) of pose change.

mode	a				b				c			
	1		2		1		2		1		2	
	X	Y	X	Y	X	Y	X	Y	X	Y	X	Y
X	-sin(20)	0	-sin(40)	0	-sin(80)	0	-sin(80)	0	-sin(40)	0	-sin(20)	0
Y	cos(20)	0	cos(40)	0	cos(80)	0	-cos(80)	0	-cos(40)	0	-cos(20)	0
Z	0	1	0	1	0	1	0	1	0	1	0	1
θX	0	-Rsin(20)	0	-Rsin(40)	0	-Rsin(80)	0	-Rsin(80)	0	Rsin(40)	0	Rsin(20)
θY	0	Rcos(20)	0	Rcos(40)	0	Rcos(80)	0	-Rcos(80)	0	Rcos(40)	0	Rcos(20)
θZ	-R	0	-R	0	-R	0	-R	0	-R	0	-R	0

Table 2: Image motion on each of the 6 coarse sensors in response to motion of the segment.

The geometry of the M2 sensor is shown on the right of Figure 9. To avoid confusion, Greek letters are used to denote the 4 degrees of freedom that can be sensed in a single sensor assembly. Moving an M2 segment in 6 DOF will only affect the 3 nearest sensors. If a segment is associated with sensors a, b, and c (Figure 9), then making unit perturbations on the segment will create the signals shown in Table 3. The numbers in Table 3 assume that the spacing between the M2 segment centers is 1 meter. The units are microns (or microradian) per micron (or microradian).

	ξ_a	η_a	ψ_a	ϕ_a	ξ_b	η_b	ψ_b	ϕ_b	ξ_c	η_c	ψ_c	ϕ_c
X	-0.5		+0.866		-1				-0.5		-0.866	
Y	+0.866		+0.5				+1		-0.866		0.5	
Z		+1				-1				-1		
θX		-0.25		+0.5		+0.5		+1		+0.25		+0.5
θY		+0.433		-0.866						+0.433		0.866
θZ	-0.5				-0.5				-0.5			

Table 3: Changes in sensor displacements and rotations that result from unit perturbations of an M2 segment.

A "system matrix" is a representation of the expected sensor readings in response to a unit perturbation of each controlled degree of freedom. We are controlling 6 degrees of freedom of each outer segment, relative to the center segment, so there are 36 controlled modes in both M1 and M2. Each of the 3 metrology systems measures 48 values. (In the case of the M1 coarse system, each of the 24 cameras measures two image translation parameters.) As a result, we end up with 48 X 36 element system matrices. Since the response to movement of a generic outer segment is known, it is easy to build up system matrices simply by replicating these values, keeping track of the segment location and its neighbors. As an example, the system matrix for the M2 metrology system is shown in Figure 10, with the matrix value mapped to image intensity.

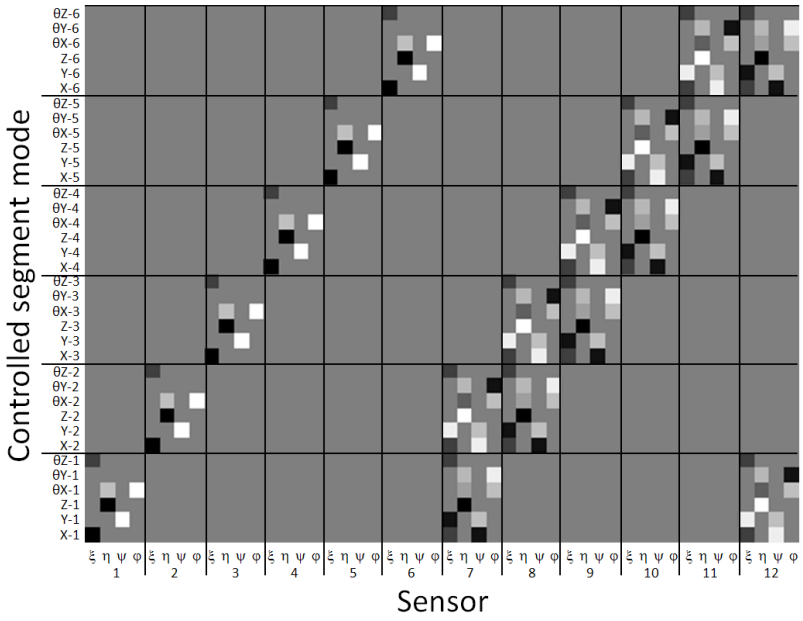

Figure 10. The system matrix for the M2 metrology system.

A singular-valued decomposition routine was applied to the 3 system matrices to analyze the natural modes of each system. None of the system matrices leads to unobservable modes. The Eigen values for the systems are plotted in Figure 11. As an example, the 36 natural modes are displayed for the M2 system in Figure 12, with the mode value mapped to intensity. The first mode is shown in the lower left corner, the last mode in the upper right. The most crucial modes for the M2 system are piston, tip, and tilt. Fortunately, these terms are represented mostly by the stronger Eigen modes.

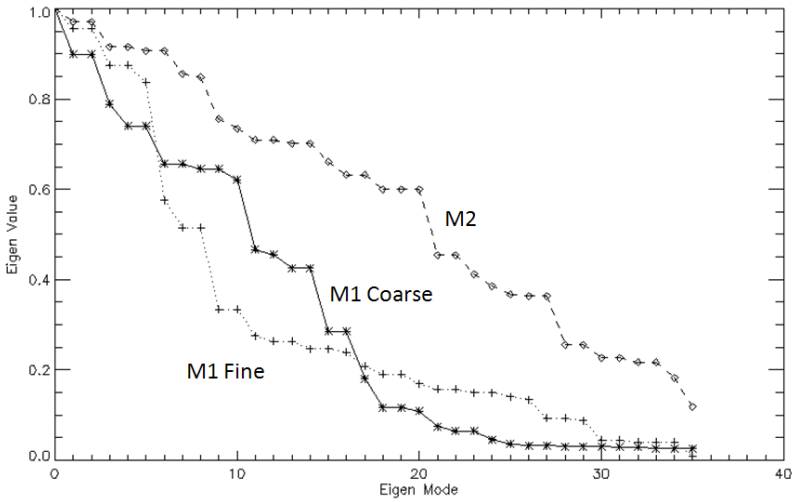

Figure 11. Relative Eigen values for the 3 metrology systems.

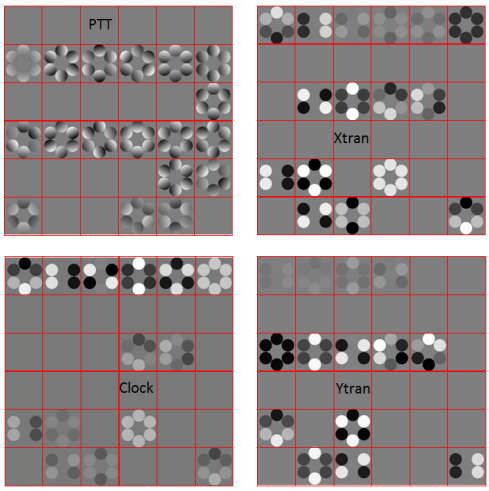

Figure 12. Eigen modes for the M2 metrology system. Each mode is the combination of the represented Piston/Tip/Tilt, X-translation, Y-translation, and clocking terms, which are mapped to intensity in the display.

5. NOISE PROPAGATION

Taking the pseudo inverse of the system matrix leads to the "control matrix" which can be used to calculate the modes associated with a given set of sensor measurements. By generating random sensor values for an input, we can use the control matrix to determine the associated segment positions that would be inferred from those values. Keeping track of the statistics in a Monte-Carlo simulation will give us a good estimate of the "noise floor" of each control system.

Recall that we are assuming the following sensitivities:

- M1 Coarse: 2 microns (long-term stability)
- M1 Fine: 1 nm
- M2: ΔX, ΔY: 0.85 nm, ΔZ: 0.6 nm, θX: 12 nRad

Using a simple Monte Carlo analysis involving 1000 random sensor realizations, the sensitivity predictions in Table 6 were generated. The only result in Table 6 that is a bit concerning is the piston sensitivity for M2 of 5.9 nm. This is

slightly over the stated goal of 5 nm (or 10 nm in the wavefront). We will need to watch this term carefully as the preliminary design is completed. As stated in Section 1, we need a long term (12 hour) stability of about 1 microradian for the tip/tilt of M2. The predicted noise floor of the M2 sensors is about 100X better than this, which is encouraging. The real issue, however, is the stability of the M2 sensors. The results shown in Table 6 for M2 were derived from the assumption that the hypothetical capacitor described in Section 2.3 has a sensitivity of 0.6 nm. Therefore, the same capacitor would need to be stable to better than 60 nm for 12 hours. Consequently, this will also be a chief consideration for the preliminary design.

	M1		M2
Mode	Coarse	Fine	
X translation	4.1 μm	0.7 nm	0.4 nm
Y translation	3.2 μm	0.6 nm	0.5 nm
Piston	4.1 μm	2.3 nm	5.9 nm
Theta-X	1.0 μRad	0.6 nRad	11.1 nRad
Theta-Y	1.4 μRad	0.5 nRad	9.5 nRad
Theta-Z	0.9 μRad	0.6 nRad	0.2 nRad

Table 3: Predicted coarse and fine sensitivity.

6. CONCLUSION

We have proposed a conceptual design of metrology systems for maintaining optical alignment of the M1 and M2 mirror segments. A first-order analysis indicates that these metrology systems will meet or exceed our alignment requirements. Upcoming design, analysis, and prototyping will refine our understanding of the expected performance.

7. ACKNOLEDGEMENTS

This work has been supported by the GMTO Corporation, a non-profit organization operated on behalf of an international consortium of universities and institutions: Astronomy Australia Ltd, the Australian National University, the Carnegie Institution for Science, Harvard University, the Korea Astronomy and Space Science Institute, the Smithsonian Institution, The University of Texas at Austin, Texas A&M University, University of Arizona and University of Chicago.

REFERENCES

[1] A. Bouchez, et al., “The Giant Magellan Telescope phasing system,” SPIE 8447-138, 2012. These proceedings.

[2] T. Mast, G. Chanan, J. Nelson, R. Minor, R. Jared, “Edge sensor design for the TMT,” Proc. SPIE 6267, 62672S, 2006.

[3] Douglas B. Leviton, Jeff Kirk and Luke Lobsinger, "Ultrahigh-resolution Cartesian absolute optical encoder", Proc. SPIE 5190, 111 (2003)

[4] Douglas B. Leviton, "Ultrahigh resolution absolute Cartesian electronic autocollimator", Proc. SPIE 5190, 468 (2003)